Korean J. Chem. Eng., 33(9), 2747-2755 (2016)
DOI: 10.1007/s11814-016-0092-8

pISSN: 0256-1115
eISSN: 1975-7220

Synthesis of metal organic framework (MOF-5) with high selectivity for CO_2/N_2 separation in flue gas by maximum water concentration approach

Ning Jiang*,, Zhiyong Deng*,**,†, Shaoying Liu*,**, Congming Tang***, and Gongying Wang*,**,†**

*Chengdu Institute of Organic Chemistry (Chengdu Organic Chemicals Co., Ltd.), Chinese Academy of Science, Chengdu, 610041, P. R. China
**University of Chinese Academy of Science, Beijing, 100049, P. R. China
***Chemical Synthesis and Pollution Control Key Laboratory of Sichuan Province, China West Normal University, Nanchong, 637002, P. R. China
(*Received 17 January 2016 • accepted 31 March 2016*)

Abstract−Water plays a crucial role in the synthesis mechanism of metal organic framework-5 (MOF-5). Synthesized MOF-5 with good phase structure and large specific surface area is largely determined by an important synthesis factor: the total water concentration of the initial synthesis solution (C_{tw}). An understanding of the effects of different and high C_{tw} on the synthesis of MOF-5 and the investigation of the maximum C_{tw} suitable for the synthesis of MOF-5 are important to guide the synthesis of MOF-5. Through the research of the maximum C_{tw}, a favorable synthetic approach was established which could realize the synthesis of MOF-5 with fine performance on CO_2 adsorption and separation. The research results show that the maximum C_{tw} could be as high as 1,440 mmol/L, and synthesized MOF-5 still has a good phase structure and a large specific surface area of 2,136 m^2/g (BET). Synthesized MOF-5 by the maximum C_{tw} exhibits a high CO_2 adsorption capacity of 2.5 mmol/g and a low N_2 adsorption capacity of 0.2 mmol/g at 298 K and 100 kPa. More importantly, synthesized MOF-5 by the maximum C_{tw} exhibits a high selectivity for CO_2/N_2 of 18-22 at 298 K and 20-130 kPa in simulated flue gas.

Keywords: Metal Organic Framework-5 (MOF-5), Water, CO_2, Adsorption, Separation

INTRODUCTION

Metal organic frameworks (MOFs), which are a class of important porous crystalline materials, exhibit large surface area and tunable properties [1,2]. They have achieved considerable attention for their potential in catalysis, magnetism, fluorescence, gas adsorption and separation [3-6], etc.

Metal organic framework-5 (MOF-5), composed by secondary building unit $Zn_4O(BDC)_3$, synthesized by zinc ion (Zn^{2+}) and terephthalic acid (H_2BDC), has been reported with a large specific surface area of 3,800 m^2/g [7]. The voluminous pore space enclosed by its supramolecular structure results in a high CO_2 adsorption capacity of 21.7 mmol/g at 298 K and 35 atm. And this value is substantially greater than many porous materials reported [8]. The ability of MOF-5 on CO_2 adsorption and separation is mainly determined by its metal active site, specific surface area, pore size and volume [9-11]. But these factors are primarily determined by two fundamental conditions: the total water concentration of the initial synthesis solution (C_{tw}) and the solvent used in the synthesis process [7,12-14].

Two kinds of water can be present in the initial synthesis solution at the same time in the synthesis of MOF-5: the crystal water of zinc nitrate (corresponding concentration, C_{cw}), and the free water of solvent (corresponding concentration, C_{fw}). But to synthesize MOF-5 with a large specific surface area and a good phase structure, the free water of solvent needed to be removed or anhydrous solvent was used in previous reports [7,15,16]. This is because MOF-5 is hydrolabile, and it is easy to adsorb the free water, which will make it collapse to a nonporous material ($C_{24}H_{22}O_{18}Zn_4$) [7]. Hence, prior to the synthesis of MOF-5, the free water of solvent needs to be removed by a dehydration process to eliminate the influence of the free water. This means that synthetic cost and technological process will increase. But even so, the C_{cw} used to synthesize MOF-5 by solvothermal method is also set to a low level of 100-840 mmol/L [12,15-19]. In the vast majority of previous literature, 480 mmol/L (C_{cw}) reported by Yaghi is a most commonly used parameter [19]. This is because if the C_{cw} is increased too high, then the concentration of Zn^{2+} will also be improved correspondingly, which is easy to make zincic precipitates forming.

In fact, crystal water and free water are hardly any different in the synthesis mechanism of MOF-5 [7,14,20]. And it is well known that water is a premise of the solvent (DMF or DEF) decomposing to generate a deprotonation agent (dimethylamine or diethylamine), and the deprotonation agent is a key factor for the ligand (H_2BDC) deprotonating to synthesize MOF-5 [14,20]. Meanwhile, the coordination of water to metal cation can also increase the acidity of Zn^{2+} and prevent zincic precipitates forming by a proper C_{tw} [14]. Hence, a properly high C_{tw} not only can promote the synthesis of MOF-5, but also helps to remove the dehydration process of solvent and save the synthetic cost.

†To whom correspondence should be addressed.
E-mail: zhiyongdeng@cioc.ac.cn, gywang@cioc.ac.cn

MOF-5 was synthesized by N,N-Diethylformamide (DEF) and low C_{tw}, MOF-5 usually has a large specific surface area of 2,900-3,800 m^2/g and a perfect crystal structure almost without any defect [7,8,12,21]. But the CO_2 adsorption capacity of the perfect MOF-5 is as low as 0.8-1.1 mmol/g at 298 K and 100 kPa [8,11,16,22,23], and its selectivity for CO_2/N_2 is also less than 5 at 298 K and 0-4.5 MPa in simulated flue gas [24-26]. MOF-5 was synthesized by N,N-Dimethylformamide (DMF) and low C_{tw}, MOF-5 usually has a smaller specific surface area of 600-1,300 m^2/g, and some defects inevitably exist in its crystal structure [12,13]. But when the C_{tw} is greater than or equal to 840 mmol/L, the specific surface area of the defective MOF-5 can reach more than 2,000 m^2/g [17,27], and its CO_2 adsorption capacity could be as high as 2.1 mmol/g at 298 K and 100 kPa [17,18]. Advances in the synthetic approach of MOF-5 like these suggest that further appropriate increase in C_{tw} and using DMF as solvent are beneficial to enhance the ability of MOF-5 on CO_2 adsorption and separation.

Although pure MOF-5 is unstable to moisture in the atmosphere, MOF-5 doped by a certain amount of nickel (Ni) is stable. MOF-5 with nickel exposed in humid air for seven days still has a high H_2 absorption capacity, and its phase structure and performance of nitrogen adsorption-desorption are almost without any changes [28]. Since moisture-stable MOF-5 was discovered, MOF-5 potentially could be applied to the separation of CO_2 in flue gas, which makes the research of MOF-5 important. As reported in the literature [28], moisture-stable MOF-5 was synthesized by the equal amount of zinc nitrate hexahydrate and nickel nitrate hexahydrate, and two nitrates brought the crystal water in the initial synthesis solution. In addition, it is well known that the C_{tw} is set too high, for example 2,015 mmol/L around, then imporous MOF-69C will be synthesized [29]. So, to avoid the growth of other non-porous crystals ($C_{24}H_{22}O_{18}Zn_4$ and MOF-69C), the maximum C_{tw} needs to be primarily determined. And to ensure that the MOF-5 crystals were synthesized as many as possible in per unit solvent, the maximum C_{tw} also needs to be primarily determined. But at least up to now, the data reported by literature about the effects of the different and high C_{tw} on the synthesis of MOF-5 are very few, just only one [14]. And the maximum C_{tw} used to synthesize MOF-5 with a big specific surface area and a good phase structure still has not been discussed and reported.

Therefore, an understanding of the effects of the different and high C_{tw} on the synthesis of MOF-5 is important to guide the synthesis of MOF-5 and to establish a favorable synthetic approach for improving the ability of MOF-5 on CO_2 adsorption and separation. The investigation of the maximum C_{tw} suitable for the synthesis of MOF-5 could provide an important reference for the synthesis of moisture-stable MOF-5 and other modified MOF-5.

In this paper, we have studied the effects of the different and high C_{tw} on the synthesis of MOF-5 by injecting the deionized water into the initial synthesis solution in detail. And the C_{cw} was also set to a low level of 180 mmol/L in our experiments to reduce the influence of the crystal water. We also investigated the pure CO_2 and N_2 adsorption capacities of the synthesized samples, and the separation performance of the synthesized MOF-5 by the maximum C_{tw} for CO_2/N_2 in simulated flue gas. These works aim to investigate the important maximum C_{tw} suitable for the synthesis of MOF-5, and establish a new favorable synthetic approach for improving the ability of MOF-5 on CO_2 adsorption and separation.

EXPERIMENTAL

1. Crystal Synthesis

Terephthalic acid (H_2BDC, ≥99.0%), zinc nitrate hexahydrate ($Zn(NO_3)_2{\cdot}6H_2O$, ≥99.5%), N,N-Dimethylformamide (DMF, ≥99.5%), dichloromethane (CH_2Cl_2, ≥99.5%). Prior to the synthesis of the crystals, all solvents (DMF and CH_2Cl_2) were dehydrated by zeolite 4A. Crystals were synthesized following the optimized mole ratio of raw material ($Zn^{2+}:BDC^{2-}=3:1$) reported by Yaghi [19]. Zinc nitrate hexahydrate (1.5 mmol) and H_2BDC (0.5 mmol) were dissolved in DMF with 100 ml glass vials. Then a different amount of deionized water was quickly added to the vials. Including the amount of the crystal water of zinc nitrate hexahydrate, the total water concentration of the initial synthesis solution (C_{tw}) was 1,440, 1,620, 1,800, 1,980 and 2,160 mmol/L, respectively. All vials were sealed and placed in an oil bath with a uniform heating rate of 4 K/min, until the temperature of the oil bath reached 363 K and was held for 10-12 hours. The cooling rate was 2 K/min, until the temperature dropped to 333 K. To obtain a dry environment, all vials were transferred into an infrared drying oven. The solvent was quickly poured out, and the crystals were washed three times with fresh dehydration DMF, then left to soak for 12 hours. This soaking procedure was also repeated three times, and the same for the following CH_2Cl_2. Afterwards, the vials were put into a vacuum drying oven, and kept at 403 K for 10 hours. Thus samples were obtained.

2. Crystal Characterization

The samples were characterized by powder X-ray diffraction with a Cu-Kα radiation (PXRD, DMAX/Ultima IV, Rigaku Corporation, Japan). The geometric size and microstructure of the crystals were examined using a digital optical microscope (MIC, XSP-35TV, Phenix Optical, China). The specific surface area of the samples was measured through nitrogen adsorption at 77 K by Quantachrome instrument (Autosorb-IQ-MP, America). Before adsorption, each sample was treated at 393 K under high vacuum for 6 hours, then the specific surface area was calculated by the Brunauer-Emmett-Teller (BET) method, and the pore volume and pore diameter distribution of the samples were analyzed by the density functional theory (DFT).

3. Gas Adsorption and Separation

Gas adsorption and separation tests were carried out with a static gas adsorption analyzer (Fig. 1(a)) and a dynamic gas separation analyzer (Fig. 1(b)), respectively. The measuring range of all pressure sensors was 0-1,000 kPa, and the accuracy was ±0.3%. High-purity CO_2 (≥99.999%), N_2 (≥99.999%), He (≥99.999%), and the correct mixture with a composition simulated flue gas (component mole ratio, $nHe:nN_2:nCO_2=80:16:4$, Southwest Research & Design Institute of the Chemical Industry, China) were used as the gas sources.

The analytical method for the adsorption capacity of pure gas (CO_2, N_2) was as follows. According to the gas state equation ($PV=ZnRT$, Z, compressibility factor) and mass balance principle, the equilibrium gas adsorption isotherms were measured using the static

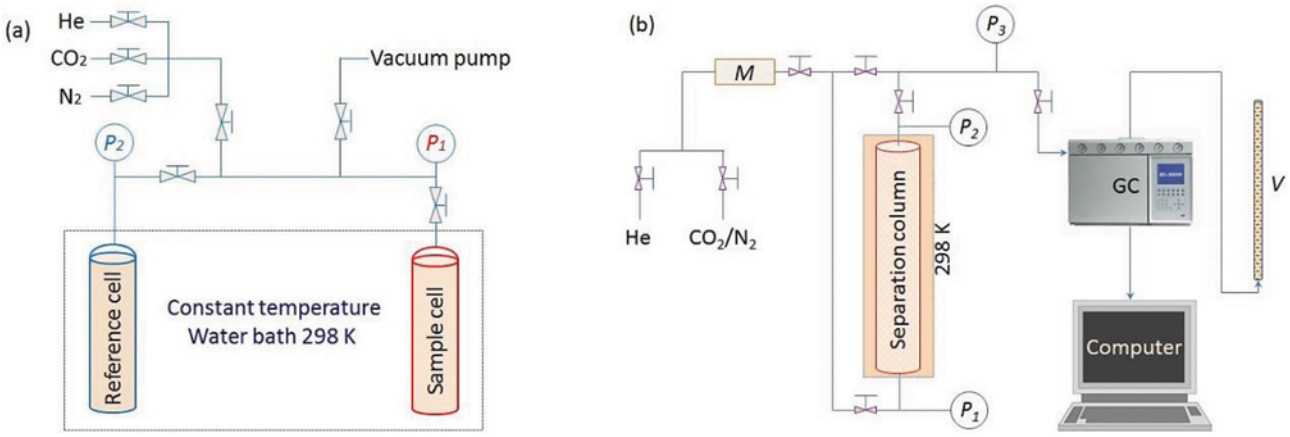

Fig. 1. Schematic diagram of static gas adsorption analyzer for (a), schematic diagram of dynamic gas separation analyzer for (b); M, mass flow meter; V, bubble flow meter; GC, gas chromatography with TCD detector.

volumetric method reported by Yaghi etc. [30]. And static volumetric method had been used successfully in previous literature [30-34]. In this method, assuming that the amount of helium adsorbed is negligible, the void volume of the sample cell (Fig. 1(a)) after adding materials was determined by injecting a known quantity of helium from the reference cell (Fig. 1(a)). Therefore, the amount of adsorbed gas (CO_2, N_2) could be calculated by formulas (1) and (2) [30].

$$m \cdot n_{ads,k} = n_{inj,k} - n_{void,k} \tag{1}$$

$$n_{inj,k} = \frac{P_{2,k} V_{rc}}{Z_k R T_2} - \frac{P'_{2,k} V_{rc}}{Z'_k R T'_2} \tag{2}$$

Herein, m is the adsorbent mass (g); $n_{ads,k}$ is the adsorption capacity of pure gas k (mmol/g); $n_{inj,k}$ is the amount of injected pure gas k (mmol); $n_{void,k}$ is the amount of unabsorbed pure gas k in the void volume of the sample cell (mmol); V_{rc} is the volume of reference cell (ml); R is molar gas constant (8.3145 J/mol/K), P_2, T_2, Z_k and P'_2, T'_2, Z'_k are the pressure (kPa), temperature (K) and compression factor of pure gas k at equilibrium in the reference cell before and after injecting the sample cell.

The analytical method for the dynamic adsorption capacity and selectivity (CO_2/N_2) was as follows. For a given separation column, and according to the mass balance principle and breakthrough curves of binary or ternary gas mixture, the dynamic adsorption capacity of component k could be calculated by formula (3) [35, 36]. Then, the selectivity or separation factor ($S_{i/j}$) between components i and j could be defined by formula (4) [35,36].

$$m \cdot n_{ads,k} = \int_0^t \mu_{in} \cdot A \cdot C_0 \cdot y_{in,k} dt - \int_0^t \mu_{out} \cdot A \cdot C_0 \cdot y_{out,k} dt - V_{void} \cdot C_{equ} \cdot y_{in,k} \tag{3}$$

$$S_{i/j} = \frac{(n/y)_i}{(n/y)_j} \tag{4}$$

where m is the adsorbent mass (g); $n_{ads,k}$ is the dynamic adsorption capacity of component k (mmol/g); μ_{in} and μ_{out} are the total linear flow speed of gas mixture at the inlet and outlet of the separation column, respectively (cm/min); A is the section area of the internal diameter of the separation column (cm^2); C_0 is the total initial concentration of gas mixture (mmol/ml); $y_{in,k}$ and $y_{out,k}$ are the mole fraction of component k in gas mixture at the inlet and outlet of the separation column, respectively (−); V_{void} is the void volume of the separation column (ml); C_{equ} is the equilibrium concentration of gas mixture of the separation column (mmol/ml). $S_{i/j}$ is the selectivity or separation factor between components i and j (−); n_i and n_j are the dynamic adsorbed amounts of component i and j, respectively (mmol/g); y_i and y_j are the mole fraction of i and j in gas phase (−).

RESULTS AND DISCUSSION

1. Crystal Phase Structure

Fig. 2 shows the PXRD patterns of the samples synthesized by different and high C_{tw}. Samples in Fig. 2(a) were synthesized at 363 K and 10 hours, but in Fig. 2(b) were synthesized at 363 K and 12 hours. Fig. 2 shows that the maximum C_{tw} suitable for the synthesis of MOF-5 with a good phase structure was 1,440 mmol/L.

C_{tw}=1,440 mmol/L, Fig. 2(a) shows that the synthesized sample had some typical characteristic peaks of MOF-5 (marked as β), and the crystal faces were clearly marked in the different diffraction directions, such as (200), (220), (400), (420). But an unknown characteristic peak on 6.5° (2θ) also shows that there is an unknown phase (marked as α) in the sample. This indicates that there are two kinds of phase structures (α, MOF-5) in the sample. Fig. 2(b) shows that the characteristic peak of 6.5° (2θ) could be completely eliminated, and MOF-5 with a good phase structure could be synthesized. This indicates that α could be transformed into MOF-5 by prolonging the synthesis time to 12 hours.

C_{tw}=1,620-1,800 mmol/L, Fig. 2(a) shows that that the synthesized samples still had several characteristic peaks of MOF-5, and the crystal faces could still be found, such as (200), (220), (400), (420). But a new characteristic peak on 8.9° (2θ) also shows a new phase exists in the samples. This reason was that the MOF-5 crystals were exposed in humid air or synthesized by an over high C_{tw}, which makes it easy to transform into imporous $C_{24}H_{22}O_{18}Zn_4$

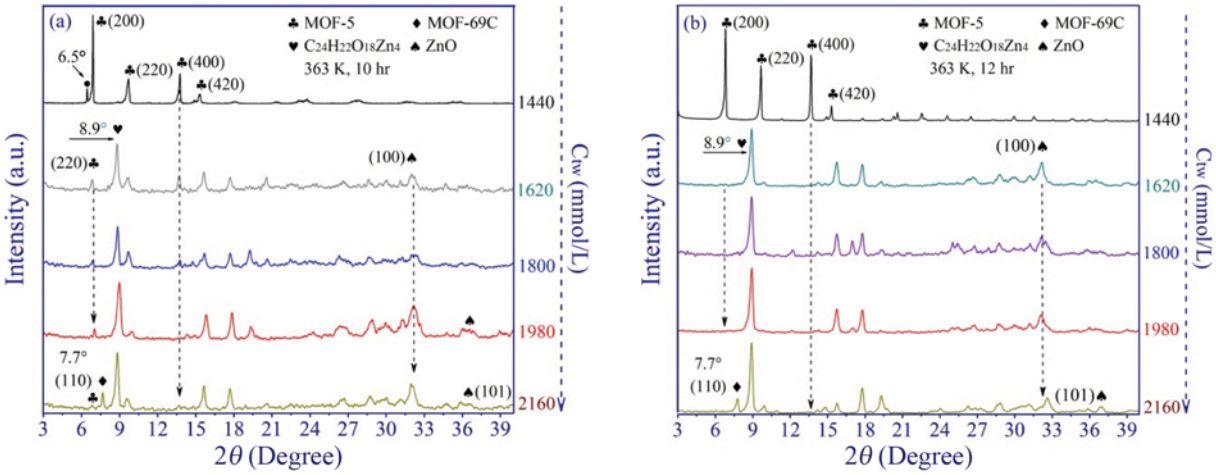

Fig. 2. PXRD patterns of samples, samples synthesized at 363 K for 10 (a) and 12 hours (b), phase structure of MOF-69C from Yaghi [14,29], phase structure of ZnO from PXRD standard pattern (PDF# 36-1451).

(marked as γ) [7,37] Interestingly, MOF-5, doped by a certain amount of nickel (Ni) and exposed in humid air for seven days, still had a high H_2 absorption capacity; and its phase structure was almost without any changes [28]. At the same time, two characteristic peaks of ZnO (marked as ζ) with the crystal face (100) and (101) could also be found. This indicates that there are three kinds of phase structures (MOF-5, $C_{24}H_{22}O_{18}Zn_4$ and ZnO) in these samples. Fig. 2(b) shows that the primary characteristic peak of MOF-5 on 6.8° (2θ) had been completely eliminated by prolonging the synthesis time to 12 hours. This indicates that synthesized MOF-5 had been completely transformed into $C_{24}H_{22}O_{18}Zn_4$. And there are only two kinds of phase structures ($C_{24}H_{22}O_{18}Zn_4$ and ZnO) in these samples.

C_{tw}=2,160 mmol/L, Fig. 2(a) shows that the synthesized sample had four types of characteristic peaks: MOF-5, MOF-69C (marked as δ), $C_{24}H_{22}O_{18}Zn_4$ and ZnO simultaneously. This indicates that there are four kinds of phase structures, and a small amount of MOF-5 still exists in the sample. Fig. 2(b) shows that any characteristic peaks of MOF-5 could not be found in the sample by prolonging the synthesis time to 12 hours. This indicates that the frameworks of MOF-5 had completely collapsed, and synthesized MOF-5 had been transformed into other materials. By this time, there are only three kinds of phase structures (MOF-69C, $C_{24}H_{22}O_{18}Zn_4$, ZnO) in the sample, and each one of them is imporous.

2. Crystal Microstructure

Fig. 3 shows the microstructures of the crystals synthesized at 363 K for 10 (a)-(e) and 12 (A)-(E) hours by different and high C_{tw}. When the C_{tw} was 1,440 mmol/L and synthesis time was 12 hours, the MOF-5 crystals with a fine crystallinity and dispersity, a single cubic shape and an average size of 30-50 μm, could be synthesized at 363 K.

C_{tw}=1,440 mmol/L: Fig. 3(a) shows that two kinds of crystals were synthesized in the sample simultaneously. One was small cube-shaped crystals (β) with an average size of 30-50 μm; the other was large rectangle-shaped crystals (α) with an average size greater than 100 μm. And the crystal-β growing in and out of the crystal-α could be observed clearly. Fig. 3(A) shows that the crystal-α could be completely eliminated by prolonging the synthesis time to 12 hours, and single cube-shaped crystals (β, MOF-5) could be synthesized. This indicates that the crystal-α is indeed a kind of transitional crystal and can be transformed into MOF-5. The results of the microstructures are consistent with the PXRD analysis (Fig. 2(a), 2(b), C_{tw}=1,440 mmol/L).

C_{tw}=1,620-1,980 mmol/L: Fig. 3(b)-(d) show that the cube-shaped crystals (β, MOF-5) and irregular block-shaped crystals (γ, $C_{24}H_{22}O_{18}Zn_4$) were synthesized in each sample simultaneously. Fig. 3(B)-(D) show that the majority of the synthesized crystals in each sample were irregular block-shaped crystals by prolonging the synthesis time to 12 hours. This indicates that the cube-shaped crystals could be transformed into the irregular block-shaped crystals by prolonging the synthesis time.

C_{tw}=2,160 mmol/L: Fig. 3(e) shows that a few rod-shaped crystals (δ, MOF-69C) were synthesized in the sample. Fig. 3(E) shows that the irregular block-shaped crystals, rod-shaped crystals and black precipitates without light transmission were synthesized simultaneously, but the cube-shaped crystals could hardly be found by prolonging the synthesis time. This indicates that an over high C_{tw} was not conducive to the synthesis of MOF-5 with a good microstructure. In fact, this experimental C_{tw} is very close to the water concentration used for the synthesis of MOF-69C [29].

3. Specific Surface Area and Pore

Table 1 is the specific surface area of the samples synthesized at 363 K for 10-12 hours by different and high C_{tw}. Table 1 shows that the maximum C_{tw} suitable for the synthesis of MOF-5 with a big specific surface area was 1,440 mmol/L.

C_{tw}=1,440 mmol/L: Table 1 shows that the specific surface area of the MOF-5 synthesized at 363 K for 12 hours could reach up to 2,136 m^2/g. This value is close to the result reported by Yaghi etc. [17,38,39]. But the specific surface area of the sample synthesized at 363 K for 10 hours was only 801 m^2/g. This reason was that the transitional crystal-α and MOF-5 simultaneously exist in the sample, which also suggests the specific surface area of the crystal-α is less than MOF-5.

C_{tw}=1,620-1,980 mmol/L: Table 1 shows that the specific surface area of the samples synthesized at 363 K for 10 hours was 823-

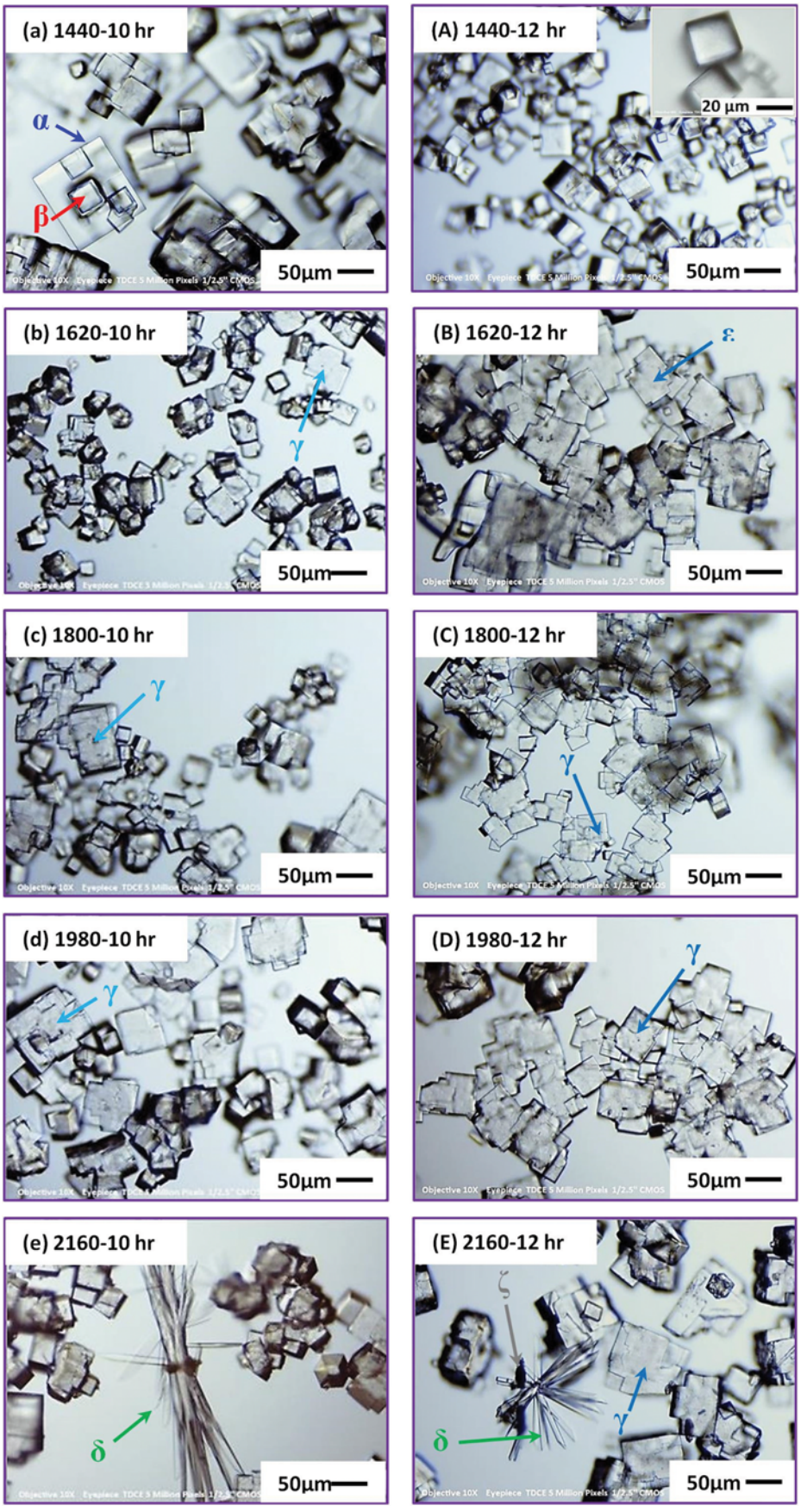

Fig. 3. Microstructures of crystals with DMF, crystals synthesized at 363 K for 10 (a)-(e) and 12 (A)-(E) hours.

Table 1. Specific surface area of samples synthesized by different C_{tw}

Synthesis time (hr)	10					12				
C_{tw} (mmol/L)	1440	1620	1800	1980	2160	1440	1620	1800	1980	2160
Phase composition	α, β	β, γ, ζ	β, γ, ζ	β, γ, ζ	β, γ, δ, ζ	β	γ, ζ	γ, ζ	γ, ζ	γ, δ, ζ
BET (m^2/g)	801	876	823	925	283	2136	33	28	17	9

α, a kind of crystal transforming into MOF-5; β, MOF-5; γ, $C_{24}H_{22}O_{18}Zn_4$; δ, MOF-69C; ζ, ZnO

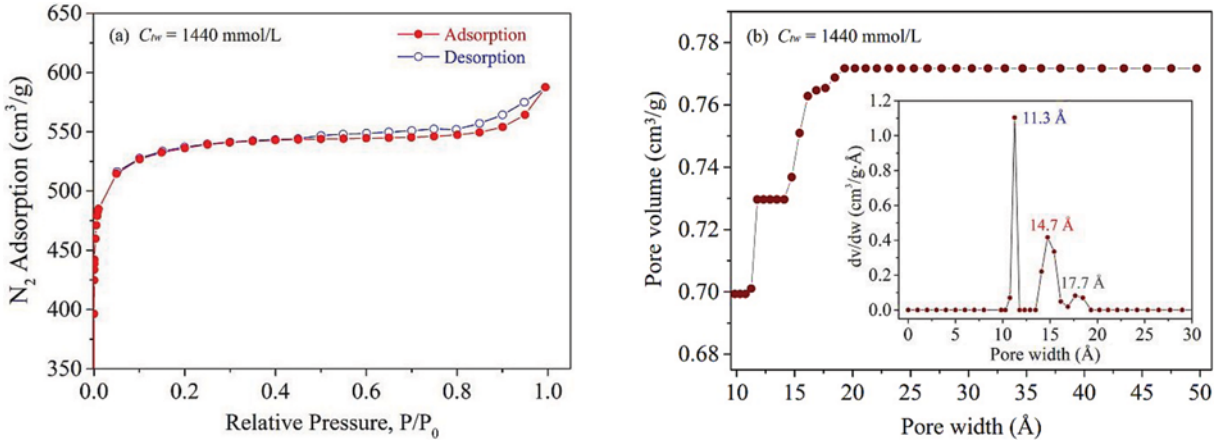

Fig. 4. N_2 adsorption and desorption isotherms (77 K) of MOF-5 for (a), pore volume and pore diameter distribution of MOF-5 for (b), MOF-5 synthesized by maximum C_{tw} of 1,440 mmol/L.

925 m^2/g and irregular. This indicates that some MOF-5 still existed in the samples, the frameworks of MOF-5 had not completely collapsed, and the collapsing process was irregular. This result is consistent with the PXRD and MIC analyses. But the specific surface area of the synthesized samples was low to 17-33 m^2/g by prolonging the synthesis time to 12 hours. This indicates that the amount of MOF-5 in these samples was extremely small.

C_{tw}=2,160 mmol/L: Table 1 shows that the specific surface area of the sample synthesized at 363 K for 10 hours was low to 283 m^2/g. And the specific surface area of the synthesized sample was only 9 m^2/g by prolonging the synthesis time to 12 hours. These indicate that the amount of MOF-5 in the two samples was also extremely small.

Fig. 4 is the N_2 adsorption and desorption isotherms at 77 K (Fig. 4(a)), and the pore volume and pore diameter distribution (Fig. 4(b)) of MOF-5 synthesized by the maximum C_{tw} of 1,440 mmol/L. Fig. 4(a) shows that synthesized MOF-5 had good property of N_2 adsorption-desorption. But the sharp rise in N_2 adsorption isotherm at $P/P_0 \geq 0.9$ suggests that some defects existed in the supramolecular structure of the synthesized MOF-5, inducing vacancy and pore defects. Fig. 4(b) clearly shows that synthesized MOF-5 indeed had some defects in its pore diameter distribution. And three types of micropores (11.3, 14.7 and 17.7 Å) existed in the synthesized MOF-5 simultaneously. Theoretically, perfect MOF-5 should have only one type of micropore by its single-crystal structure, and its aperture admits the passage of a sphere of minimum diameter 8.0 Å [38]. But Yaghi believes that the spheres can be overlapped and are placed at the atomic positions (Zn, H, C and O); then the diameter of the aperture will reach 11.0-15.1 Å [38]. This point is proved by following reports, and the pore diameter of MOF-5 with large specific surface area usually is 10-14 Å [16,17,38,39]. Fig. 4(b) also shows that the total micropore volume of the synthesized MOF-5 was 0.77 cm^3/g. This value is close to the result reported by literature [16,38,39]. Besides, the micropore volume of the pore diameter 11.3, 14.7 and 17.7 Å are 0.70, 0.03 and 0.04 cm^3/g, respectively. This indicates that the pore diameter 11.3 Å is the majority in all micropores. And the other two types of micropores existing in the synthesized MOF-5 were attributable to the nature of solvent (DMF); the minor phase consisted of doubly interpenetrated networks and irregular collapse of frameworks of MOF-5 [12,13]. However, these defects are beneficial to gas adsorption [12]. It suggests that the defects of the pore of the synthesized MOF-5 would be conducive to improving the ability of MOF-5 on CO_2 adsorption and separation.

4. Gas Adsorption and Separation

Fig. 5 gives the equilibrium CO_2 and N_2 adsorption isotherms of the synthesized samples. The maximum C_{tw} suitable for the synthesis of MOF-5 with a high CO_2 adsorption capacity and low N_2 adsorption capacity at 298 K and 100 kPa was 1,440 mmol/L.

C_{tw}=1,440 mmol/L: Fig. 5(a) shows that the samples synthesized at 363 K for 12 hours by DMF as solvent had a high CO_2 adsorption capacity of 2.5 mmol/g at 298 K and 100 kPa. This value calculated by the static volumetric method [30] is close to the result reported by Zhao using a gravimetric method and the DMF as solvent (2.1 mmol/g, 298 K and 100 kPa) [17,18]. It indicates that the static volumetric method used to analyze the CO_2 adsorption capacity of the synthesized MOF-5 is accurate and reliable. Interestingly, the CO_2 adsorption capacity of the MOF-5 synthesized by DMF as solvent is obviously higher than that by DEF as solvent (Fig. 5(a), 0.8-1.1 mmol/g, 298 K and 100-120 kPa [8,11,16,22,23]),

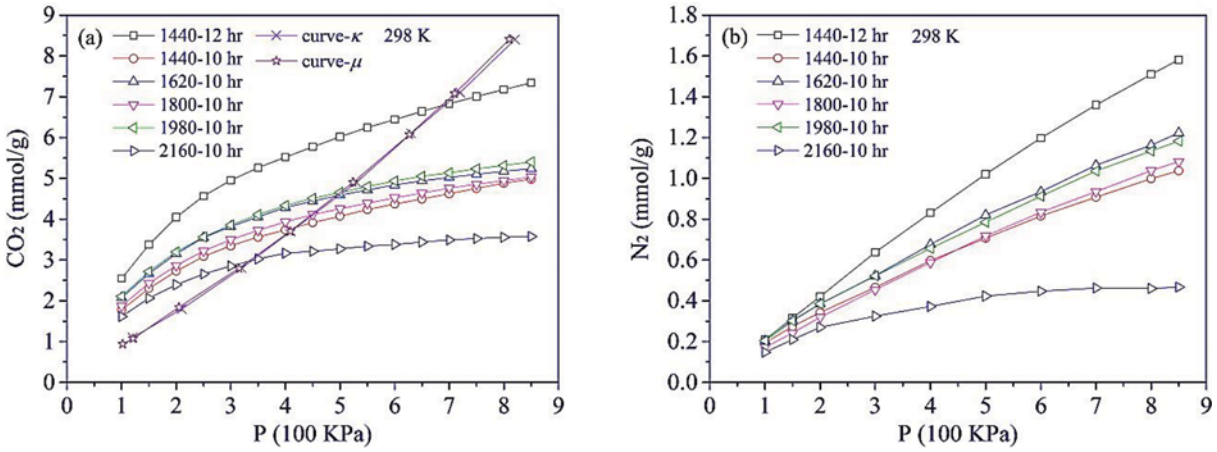

Fig. 5. Equilibrium CO_2 (a) and N_2 (b) adsorption isotherms of samples synthesized by DMF, equilibrium CO_2 adsorption isotherms of MOF-5 synthesized by DEF for curve κ and μ [8,22].

about 2-3 times. This reason was that MOF-5 synthesized by DMF usually had some defects in its phase and crystal structure, and more metal active centers (Zn) in its supramolecular structure could be exposed, which are conducive to CO_2 adsorption [12,13,16]. Besides, MOF-5 synthesized by DEF needed to be annealed at 653 K (380 °C) for 6 hours in order to make more metal active sites; then its CO_2 adsorption capacity also could reach 2.0 mmol/g at 298 K and 100 kPa [16]. But this annealing method will directly lead to the collapse of the frameworks of MOF-5, thus resulting in a low specific surface area of 988 m^2/g [16]. However, with the increase of the adsorption pressure (P_{ads}>700 kPa), the CO_2 adsorption capacity of the MOF-5 synthesized by DEF would exceed that by DMF. This reason is that MOF-5 synthesized by DEF usually has a larger specific surface area (up to 3,800 m^2/g) and a perfect crystal structure almost without any defect, which is conducive to CO_2 storage at a high pressure. Fig. 5(b) shows that the synthesized MOF-5 had a low N_2 adsorption capacity of slightly higher than 0.2 mmol/g at 298 K and 100 kPa. Besides, the ratio of adsorption capacity in theory between CO_2 and N_2 (ideal selectivity) would be reduced gradually with raising the adsorption pressure by comparing Fig. 5(a) and Fig. 5(b). Thus, a low pressure may be conducive to the separation of CO_2 in flue gas.

C_{tw}=1,620-1,980 mmol/L: Fig. 5(a) shows that the synthesized samples still had good CO_2 adsorption capacities, about 1.9-2.1 mmol/g at 298 K and 100 kPa. But the increase of adsorption pressure easily makes the CO_2 adsorption isotherms smooth, which indicates that the CO_2 adsorption capacities of these samples had approached their saturation. Fig. 5(b) shows that these samples also had a low N_2 adsorption capacity of 0.2 mmol/g around at 298 K and 100 kPa.

C_{tw}=2,160 mmol/L: Fig. 5(a)-(b) show that the synthesized sample had a very low CO_2 and N_2 adsorption capacity, indicating that the amount of MOF-5 in this sample was very little, and imporous materials were in the majority.

Fig. 6 shows the breakthrough curves of CO_2 and N_2 at 298 K with the total feed pressure 100 kPa (a) and 650 kPa (b). To test the separation performance of the MOF-5 synthesized by maximum C_{tw} of 1,440 mmol/L for CO_2/N_2 in simulated flue gas, a fixed-bed reactor was employed to obtain the breakthrough curves. In addition, to obtain the breakthrough curves at a low feed pressure, helium was used as a balance and diluent gas, and the feeding gas mixture

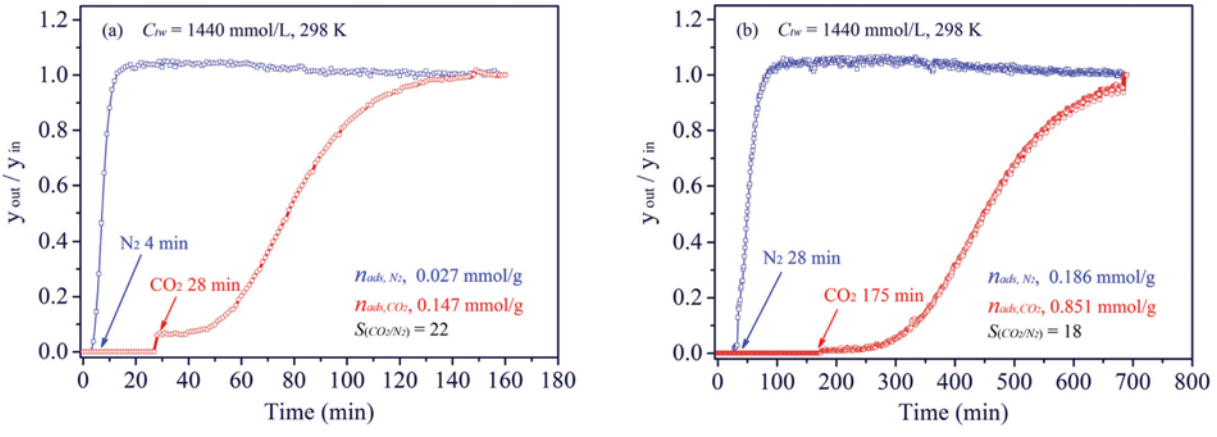

Fig. 6. Breakthrough curves of CO_2 and N_2, total feed pressure 100 kPa for (a) and 650 kPa for (b), and total flow rate of gas mixture for 10 ml/min.

had a fixed composition (component mole ratio, $nHe : nN_2 : nCO_2$= 80 : 16 : 4).

Total feed pressure was 100 kPa, the partial pressure of N_2 and CO_2 was 16 and 4 kPa, respectively, and the total partial pressure of N_2 and CO_2 was 20 kPa. Fig. 6(a) shows that the synthesized MOF-5 by the maximum C_{tw} of 1,440 mmol/L exhibited a high selectivity for CO_2/N_2 of 22 at 298 K. And the initial breakthrough time of N_2 (4 min) was earlier than CO_2 (28 min), and the amount of adsorbed N_2 (0.027 mmol/g) was clearly less than CO_2 (0.147 mmol/g).

Total feed pressure was 650 kPa, the partial pressure of N_2 and CO_2 was 104 and 26 kPa, respectively, and the total partial pressure of N_2 and CO_2 was 130 kPa being close to the real pressure of the flue gas. Fig. 6(b) shows that the synthesized MOF-5 by the maximum C_{tw} of 1,440 mmol/L still exhibited a fine selectivity for CO_2/N_2 of 18 at 298 K. And the initial breakthrough time of N_2 (28 min) was also earlier than CO_2 (175 min); the amount of adsorbed N_2 (0.186 mmol/g) was still less than CO_2 (0.851 mmol/g). So the competitive adsorption was still strong between CO_2 and N_2 even if the total feed pressure was increased to 650 kPa. But the selectivity for CO_2/N_2 would decrease with raising the total feed pressure by comparing Fig. 6(a) and Fig. 6(b). This result is consistent with the analysis of the ideal selectivity (CO_2/N_2) by comparing Fig. 5(a) and 5(b). Besides, the dynamic adsorption capacity of N_2 at its partial pressure 104 kPa (Fig. 6(b)) was less than and close to the value of the static adsorption capacity of pure N_2 at 100 kPa (Fig. 5(b), 0.2 mmol/g). This indicates that the static volumetric method and dynamic method employed to analyze the gas adsorption capacity of the synthesized MOF-5 are all accurate and reliable.

Furthermore, a high mole ratio between component N_2 and CO_2 ($nN_2 : nCO_2 \geq 1 : 1$) is not conducive to the separation of CO_2 and N_2 using perfect MOF-5, and the selectivity for CO_2/N_2 is less than 5 at 298 K and a given feed pressure of 0-4.5 MPa [24-26]. And only when the gas mixture had a high proportion of component CO_2 (mole ratio, $nN_2 : nCO_2 < 2 : 8$), could be the selectivity for CO_2/N_2 increased to 14-60 [18,24]. Interestingly, MOF-5 with some defects in its pores (Fig. 4(b)) had a high selectivity for CO_2/N_2 of 18-22 at 298 K and partial pressure 20-130 kPa. This indicates that some defects in the structure of the synthesized MOF-5 are indeed helpful to the separation of CO_2 and N_2.

CONCLUSIONS

We studied the effects of the different and high C_{tw} on the synthesis of MOF-5 in detail, investigated the maximum C_{tw} suitable for the synthesis of MOF-5, and established a favorable synthetic approach for improving the ability of MOF-5 on CO_2 adsorption and separation. The research results show that the maximum C_{tw} suitable for the synthesis of MOF-5 could be as high as 1,440 mmol/L. MOF-5 synthesized by the maximum C_{tw} and DMF as solvent still had a good phase structure, a fine microstructure and a large specific surface area of 2,136 m^2/g (BET). Also, synthesized MOF-5 exhibited a high CO_2 adsorption capacity of 2.5 mmol/g and low N_2 adsorption capacity of 0.2 mmol/g at 298 K and 100 kPa. Interestingly, although MOF-5 synthesized by maximum C_{tw} of 1,440 mmol/L and DMF inevitably had some defects in its pores, the defective MOF-5 exhibited a high selectivity for CO_2/N_2 of 18-22 at 298 K and 20-130 kPa in simulated flue gas, which is greater than the result of less than 5 reported by the literature. Furthermore, the investigation of the C_{tw} provided some important information for the synthesis of MOF-5. Further, a reasonable increase in C_{tw} and using DMF as solvent could make some defects in the structure of MOF-5, which is indeed beneficial to enhance the ability of MOF-5 on CO_2 adsorption and separation. And the maximum C_{tw} used for the synthesis of MOF-5 should be less than or equal to 1,440 mmol/L, and an overly high C_{tw} would result in the collapse of the frameworks of MOF-5, the decrease of the specific surface area of MOF-5, and ultimately lead to MOF-5 completely transforming into some imporous materials ($C_{24}H_{22}O_{18}Zn_4$, MOF-69C).

ACKNOWLEDGEMENTS

This work was supported partially by the National Key Technology R&D Program (Grant No. 2013BAC11B05) and 1000 Talents Program of Sichuan and Talents program of Chengdu, China.

REFERENCES

1. H. Furukawa, N. Ko, Y. B. Go, N. Aratani, S. B. Choi, E. Choi, A. Ö. Yazaydin, R. Q. Snurr, M. O'Keeffe, J. Kim and O. M. Yaghi, *Science*, **329**, 424 (2010).
2. H. Deng, C. J. Doonan, H. Furukawa, R. B. Ferreira, J. Towne, C. B. Knobler, B. Wang and O. M. Yaghi, *Science*, **327**, 846 (2010).
3. X. Zhou, Y. Zhang, X. Yang, L. Zhao and G. Wang, *J. Mol. Catal. A: Chem.*, **361**, 12 (2012).
4. A. S. Munn, G. J. Clarkson, F. Millange, Y. Dumont and R. I. Walton, *Cryst. Eng. Commun.*, **15**, 9679 (2013).
5. C. A. Kent, D. M. Liu, A. Ito, T. Zhang, M. K. Brennaman, T. J. Meyer and W. B. Lin, *J. Mater. Chem. A*, **1**, 14982 (2013).
6. H. C. Yoon, P. B. S. Rallapalli, S. S. Han, H. T. Beum, T. S. Jung, D. W. Cho, M. Ko and J. N. Kim, *Korean J. Chem. Eng.*, **12**, 2501 (2015).
7. S. S. Kaye, A. Dailly, O. M. Yaghi and J. R. Long, *J. Am. Chem. Soc.*, **129**, 14176 (2007).
8. A. R. Millward and O. M. Yaghi, *J. Am. Chem. Soc.*, **127**, 17998 (2005).
9. M. Eddaoudi, J. Kim, N. Rosi, D. Vodak, J. Wachter, M. O'Keeffe and O. M. Yaghi, *Science*, **295**, 469 (2002).
10. M. L. Drummond, T. R. Cundari and A. K. Wilson, *J. Phys. Chem. C*, **117**, 14717 (2013).
11. X. Kong, H. Deng, F. Yan, J. Kim, J. A. Swisher, B. Smit, O. M. Yaghi and J. A. Reimer, *Science*, **341**, 882 (2013).
12. C. S. Tsao, M. S. Yu, T. Y. Chung, H. C. Wu, C. Y. Wang, K. S. Chang and H. L. Chen, *J. Am. Chem. Soc.*, **127**, 15997 (2009).
13. J. Hafizovic, M. Bjørgen, U. Olsbye, P. D. C. Dietzel, S. Bordiga, C. Prestipino, C. Lamberti and K. P. Lillerud, *J. Am. Chem. Soc.*, **129**, 3612 (2007).
14. S. Hausdorf, J. Wagler, R. Mossig and F. O. R. L. Mertens, *J. Phys. Chem. A*, **112**, 7567 (2008).
15. J. L. C. Rowsell, E. C. Spencer, J. Eckert, J. A. K. Howard and O. M. Yaghi, *Science*, **309**, 1350 (2005).
16. S. Gadipelli and Z. Guo, *Chem. Mater.*, **26**, 6333 (2014).

17. Z. Zhao, Z. Li and Y. S. Lin, *Ind. Eng. Chem. Res.*, **48**, 10015 (2009).
18. Z. Zhao, X. Ma, A. Kasik, Z. Li and Y. S. Lin, *Ind. Eng. Chem. Res.*, **52**, 1102 (2013).
19. O. M. Yaghi, M. Eddaoudi, H. Li, J. Kim and N. Rosi, United States Patent, No., 2003/0004364 A1 (2003).
20. S. Hausdorf, F. Baitalow, J. Seidel and F. O. R. L. Mertens, *J. Phys. Chem. A*, **111**, 4259 (2007).
21. O. M. Yaghi and Q. W. Li, *MRS Bull.*, **34**, 682 (2009).
22. K. S. Walton, A. R. Millward, D. Dubbeldam, H. Frost, J. J. Low, O. M. Yaghi and R. Q. Snurr, *J. Am. Chem. Soc.*, **130**, 406 (2008).
23. D. Saha, Z. Bao, F. Jia and S. Deng, *Environ. Sci. Technol.*, **44**, 1820 (2010).
24. J. R. Karra and K. S. Walton, *J. Phys. Chem. C*, **114**, 15735 (2010).
25. B. Liu and B. Smit, *Langmuir*, **25**, 5918 (2009).
26. S. Keskin and D. S. Sholl, *Ind. Eng. Chem. Res.*, **48**, 914 (2009).
27. L. Zhang and Y. H. Hu, *Mater. Sci. Eng., B*, **176**, 573 (2011).
28. H. Li, W. Shi, K. Zhao, H. Li, Y. Bing and P. Cheng, *Inorg. Chem.*, **51**, 9200 (2012).
29. N. L. Rosi, J. Kim, M. Eddaoudi, B. Chen, M. O'Keeffe and O. M. Yaghi, *J. Am. Chem. Soc.*, **127**, 1504 (2005).
30. A. G. Wong-Foy, A. J. Matzger and O. M. Yaghi, *J. Am. Chem. Soc.*, **128**, 3494 (2006).
31. P. Baran, K. Zarębska and M. Bukowska, *Energy Fuels*, **29**, 1899 (2015).
32. M. Sudibandriyo, Z. Pan, J. E. Fitzgerald, R. L. Robinson and Jr., K. A. M. Gasem, *Langmuir*, **19**, 5323 (2003).
33. S. A. Mohammad, J. S. Chen, J. E. Fitzgerald, R. L. Robinson and Jr., K. A. M. Gasem, *Energy Fuels*, **23**, 1107 (2009).
34. S. A. Mohammad, A. Arumugam, R. L. Robinson and Jr., K. A. M. Gasem, *Energy Fuels*, **26**, 536 (2012).
35. Q. Wu, L. Zhou, J. Wu and Y. Zhou, *J. Chem. Eng. Data*, **50**, 635 (2005).
36. T. Remy, S. A. Peter, S. V. Perre, P. Valvekens, D. E. D. Vos, G. V. Baron and J. F. M. Denayer, *J. Phys. Chem. C*, **117**, 9301 (2013).
37. Y. Ming, J. Purewal, J. Yang, C. Xu, R. Soltis, J. Warner, M. Veenstra, M. Gaab, U. Müller and D. J. Siegel, *Langmuir*, **31**, 4988 (2015).
38. H. Li, M. Eddaoudi, M. O'Keeffe and O. M. Yaghi, *Nature*, **402**, 276 (1999).
39. M. Eddaoudi, H. Li and O. M. Yaghi, *J. Am. Chem. Soc.*, **122**, 1391 (2000).